Biochimica et Biophysica Acta 1848 (2015) 385–391

Contents lists available at ScienceDirect

Biochimica et Biophysica Acta

journal homepage: www.elsevier.com/locate/bbamem

Real-time examination of aminoglycoside activity towards bacterial mimetic membranes using Quartz Crystal Microbalance with Dissipation monitoring (QCM-D)

Tanmaya Joshi [a], Zhi Xiang Voo [a,1], Bim Graham [b], Leone Spiccia [a,*], Lisandra L. Martin [a,*]

[a] School of Chemistry, Monash University, Clayton, Victoria 3800, Australia
[b] Monash Institute of Pharmaceutical Sciences, Monash University, Parkville, Victoria 3052, Australia

ARTICLE INFO

Article history:
Received 15 June 2014
Received in revised form 3 September 2014
Accepted 14 October 2014
Available online 23 October 2014

Keywords:
Quartz crystal microbalance
Supported lipid bilayer
Aminoglycoside
Antibiotic
Molecular mechanism

ABSTRACT

The rapid increase in multi-drug resistant bacteria has resulted in previously discontinued treatments being revisited. Aminoglycosides are effective "old" antibacterial agents that fall within this category. Despite extensive usage and understanding of their intracellular targets, there is limited mechanistic knowledge regarding how aminoglycosides penetrate bacterial membranes. Thus, the activity of two well-known aminoglycosides, kanamycin A and neomycin B, towards a bacterial mimetic membrane (DMPC:DMPG (4:1)) was examined using a Quartz Crystal Microbalance with Dissipation monitoring (QCM-D). The macroscopic effect of increasing the aminoglycoside concentration showed that kanamycin A exerts a threshold response, switching from binding to the membrane to disruption of the surface. Neomycin B, however, disrupted the membrane at all concentrations examined. At concentrations above the threshold value observed for kanamycin A, both aminoglycosides revealed similar mechanistic details. That is, they both inserted into the bacterial mimetic lipid bilayer, prior to disruption via loss of materials, presumably aminoglycoside-membrane composites. Depth profile analysis of this membrane interaction was achieved using the overtones of the quartz crystal sensor. The measured data is consistent with a two-stage process in which insertion of the aminoglycoside precedes the 'detergent-like' removal of membranes from the sensor. The results of this study contribute to the insight required for aminoglycosides to be reconsidered as active antimicrobial agents/co-agents by providing details of activity at the bacterial membrane. Kanamycin and neomycin still offer potential as antimicrobial therapeutics for the future and the QCM-D method illustrates great promise for screening new antibacterial or antiviral drug candidates.

1. Introduction

The uncontrolled use of antibiotics over almost a century has resulted in bacterial mutations and resistance towards existing treatments. As a consequence, many antibiotics have been rendered ineffective and there is now an urgent need for new classes of antibiotics to combat multi-drug resistant (MDR) organisms [1]. Aminoglycosides were first introduced as antibacterial therapeutics in the 1940's as they showed activities towards both Gram-negative and Gram-positive bacteria [2]. However, with the emergence of equally potent but less toxic antibiotics, the use of aminoglycosides as antibiotics fell out of favor. But, with the increasing threat of MDR bacteria [3–7] and the decline in new antibiotics approved to help combat this global challenge [8], aminoglycosides are being revisited [9–17]. Because aminoglycosides have been able to largely evade bacterial resistance due to their waned use, it has made them a safer choice [9–17]. In particular, approaches in which aminoglycosides are used in combination therapy with other antibiotics is an emerging strategy [9–18].

Aminoglycosides [19] are a large family of amino-modified sugars, of which streptomycin is the most well-known member [20]. Two related derivatives are kanamycin A and neomycin B. A common structural feature shared by these two aminoglycosides is the presence of the central 2-deoxystreptamine (2-DOS) ring (Fig. 1). In kanamycin, the 2-DOS core is glycosylated with amino sugars at positions 4 and 6, while neomycin features amino sugars at positions 4 and 5, as shown in Fig. 1 [19].

Aminoglycosides are especially active towards Gram-negative bacteria and their primary bactericidal mode-of-action is through binding to the 16S rRNA component of the 30s subunit of the bacterial ribosome [21–23]. This causes miscoding of genetic material during the translation of mRNA in the 16S rRNA mer, thereby interfering with protein synthesis. Aminoglycosides are also capable of binding to a wide range of other RNA-based structures, including catalytic RNAs

* Corresponding authors.
E-mail addresses: Leone.Spiccia@monash.edu (L. Spiccia), Lisa.Martin@monash.edu (L.L. Martin).
[1] Current address: Institute of Bioengineering and Nanotechnology, 31 Biopolis Way, The Nanos, Singapore 138669, Singapore and NUS Graduate School for Integrative Sciences & Engineering (NGS), 28 Medical Drive, Singapore 117456, Singapore.

http://dx.doi.org/10.1016/j.bbamem.2014.10.019
0005-2736/

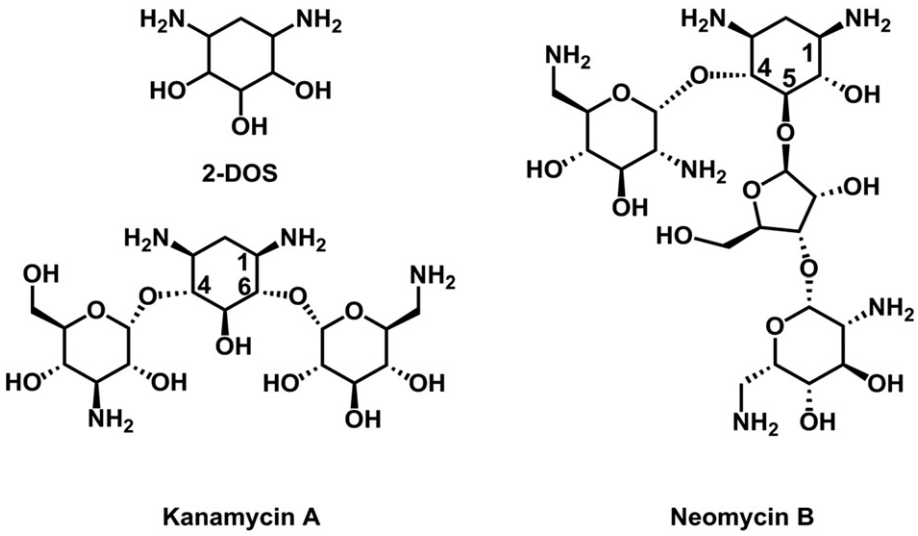

Fig. 1. Molecular structures of 2-deoxystreptamine (2-DOS), kanamycin A and neomycin B.

[24], tRNAs [19], portions of mRNA [25], and viral RNAs such as RRE [26] and Tar in HIV [27,28].

They have been found to promote the cleavage of hairpin ribozymes, to indirectly interfere with the splicing of the td intron, to act as enhancers of the catalytic properties of group I intron ribozymes, and even to inhibit ribozymes such as the hammerhead and hepatitis delta virus (HDV) ribozymes [21]. Neomycin B has also been reported to catalyze phosphodiester hydrolysis in a model RNA system, adenylyl(3′–5′)adenosine (ApA) [29], and RNA oligonucleotides [30]. However, in order for the aminoglycosides to reach these and other intracellular targets they must first penetrate the cell membrane.

Several biophysical studies have been conducted to assess the aminoglycosides' ability to permeate biological membranes [31] and phospholipids [32]. Toxicity towards cochlear [33–37] and renal cells [34,36] has been noted, with neomycin B showing the highest ototoxicity and nephrotoxicity. The fact that neomycin B has the highest positive charge among the various aminoglycosides (at physiological pH) indicates that charge may play a role in the interaction of the aminoglycosides with membranes [37–39]. Moreover, the ability of aminoglycosides to cause liposomal aggregation by binding to anionic lipid head groups via electrostatic attraction has also been documented [40–42]. Earlier studies exploring the mode of action of aminoglycosides reported blebs along the cell walls of the *Escherichia coli* bacteria after aminoglycoside administration [43,44]. More recently, it has been established that aminoglycosides can form channels or fissures in the outer cell membrane [45], allowing their influx into the cytoplasm, followed by targeting of the bacterial ribosomes. Hancock and co-workers have shown that these polycationic aminoglycosides can also be taken up across the *E. coli* outer membrane by another mechanism termed as self-promoted uptake pathway [38,39,46,47]. Despite significant knowledge of aminoglycoside intracellular activity, the mechanism of uptake of aminoglycosides is less well understood. Clearly aminoglycosides must be able to pass across the biological membrane in order to achieve effective intracellular activity.

In this study, we explore the activity of two well-known aminoglycosides, kanamycin A and neomycin B, towards bacterial mimetic membranes using a sensitive platform device: a quartz crystal microbalance with dissipation monitoring (QCM-D) [48,49]. This biophysical technique enables exploration of the membrane activity of these two aminoglycoside derivatives in real-time. Aminoglycosides are themselves facing an inevitable threat of resistance, mainly from aminoglycoside modifying enzymes (mediating selective resistance) and 16S rRNA methyltransferases (conferring class-wide resistance) [12]. Their still remain outstanding questions on the mode of action of aminoglycosides [9,11–15]. New aminoglycoside derivatives, chemically modified to circumvent resistance, can be foreseen to play an important role as antibiotics in the future [9,11–15]. The data provide additional insights that may assist medicinal chemists with the development of this next generation of aminoglycoside-based antibacterial therapeutics.

2. Experimental section

2.1. Chemicals

Neomycin B trisulfate, kanamycin A sulfate, sodium chloride, potassium phosphate monobasic and potassium phosphate dibasic, cholesterol, chloroform (≥99.8%) and methanol (≥99.9%) were all purchased from Sigma-Aldrich (St. Louis, USA) and used without purification. The synthetic phospholipid derivatives, 1,2-dimyristoyl-sn-glycero-3-phosphocholine (DMPC) and 1,2-dimyristoyl-sn-glycero-3-phospho-rac-(1-glycerol) (sodium salt) (DMPG), were purchased from Avanti Polar Lipids (Alabaster, USA) and 3-mercaptopropionic acid (MPA) from Fluka. Ultrapure water with an initial resistivity of 18.2 MΩ.cm was used for all experiments. Phosphate buffered saline solutions (20 mM KH_2PO_4 and K_2HPO_4, pH 6.9 ± 0.1) containing either 100 mM (high-salt PBS) or 30 mM (low-salt PBS) sodium chloride were prepared in water.

2.2. Instrumentation and methods

A lipid composition of DMPC/DMPG (4:1 v/v) was used for liposome preparation (see Supporting Information for details), following our previously published procedure [50,51]. The Quartz Crystal Microbalance with Dissipation Monitoring (QCM-D) measurements were performed using E4 system with flow cells (Q-Sense, Västra Frölunda, Sweden). The polished, gold-coated, AT-cut quartz chips with a fundamental oscillating frequency of *ca.* 5 MHz, were used as sensor crystals. The sensors were treated with mercaptopropionic acid to create a self-assembled carboxylate monolayer prior to the introduction of the liposomes as described in the Supporting Information. All QCM-D experiments were conducted at 19.10 ± 0.05 °C [52], in triplicate, using established experimental protocols also used for peptides–membrane interactions (see Supporting Information for details) [51, 53–55]. Concentration studies were carried out using 1, 10 and 15 μM solutions of kanamycin A and neomycin B in high-salt PBS. For a typical QCM-D experiments, the relative changes in resonance frequency (Δf)

and energy dissipation (ΔD) of the sensor were simultaneously recorded at the 1st, 3rd, 5th, 7th and 9th harmonics. The primary Δf — t and ΔD — t QCM-D data were analyzed using OriginPro 8 (OriginLab, Northampton, USA) and Δf vs ΔD graphs were used for further analysis. Data for the 1st harmonic (i.e., fundamental frequency of the crystal) were not included in the analysis as it is generally unreliable, being influenced by the flow of the solution through the QCM chamber [55]. For discussion purposes, only the 7th harmonic data plots have been presented, unless otherwise stated. A typical experiment is illustrated in Fig S1.

3. Results and discussion

The interaction of kanamycin A and neomycin B with phospholipid bilayers consisting of DMPC/DMPG (4:1) was analyzed using the QCM-D. The anionic DMPC/DMPG (4:1) lipid combination is recognized as being a good biomimetic for the prokaryotic cell membrane [56,57], particularly the Gram-positive bacterial membrane [58,59]. The frequency change (Δf) from the QCM-D is related to the change in mass [60], while the dissipation output (ΔD) can be used for the qualitative profiling of structural changes in the bilayer. A decrease in Δf value implies the addition of mass onto the sensor, whereas an increase in ΔD indicates that the lipid bilayer is becoming less rigid, loosening or thickening [60–63].

The effect of the addition of kanamycin A on the lipid membrane was followed by measuring the Δf vs. t data, which showed the concentration dependence depicted in Fig. 2. The data was normalized prior to the addition of the aminoglycoside. When introduced into the chamber at 1 μM concentration, kanamycin A was found to slowly add onto the phospholipid membrane. As can be gauged from the respective Δf — t traces (Fig. 2), the oscillation frequency of the sensor decreased with time upon addition of kanamycin A until all the solution was added (~17 min). After this time, the flow was ceased and the samples were incubated for 30 min. At higher concentrations (10 and 15 μM), however, rapid removal of material from the membrane-coated sensor occurred after the initial mass addition to ~-5 Hz. At these higher concentrations the threshold for the initial binding of kanamycin ($\Delta f \approx$ -4–5 Hz) was similar, however a second 'disruption' phase corresponding to a greater mass removal from the lipid membrane was observed at 15 μM, suggesting a concentration dependence.

A similar biphasic trend of rapid initial mass uptake and material removal thereafter was observed for neomycin B, at all the concentrations studied (Fig. 3). In contrast to kanamycin, however, there was no concentration threshold observed, although the process was characterized by insertion to 4–5 Hz, followed by disruption. Interestingly, as

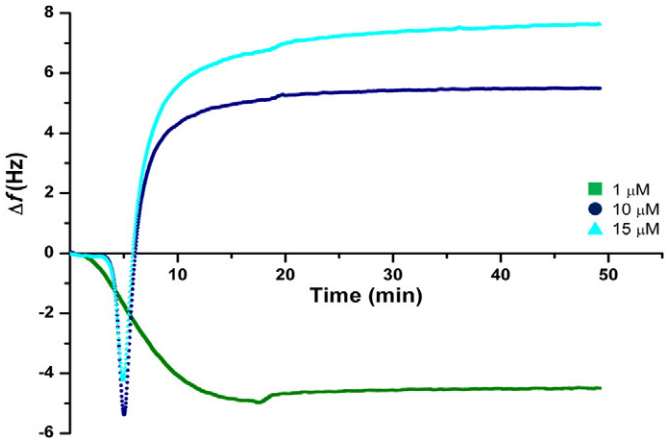

Fig. 2. Δf-t traces from QCM-D monitoring of the interaction of kanamycin A with a DMPC/DMPG (4:1) membrane showing the effect of concentration on membrane uptake.

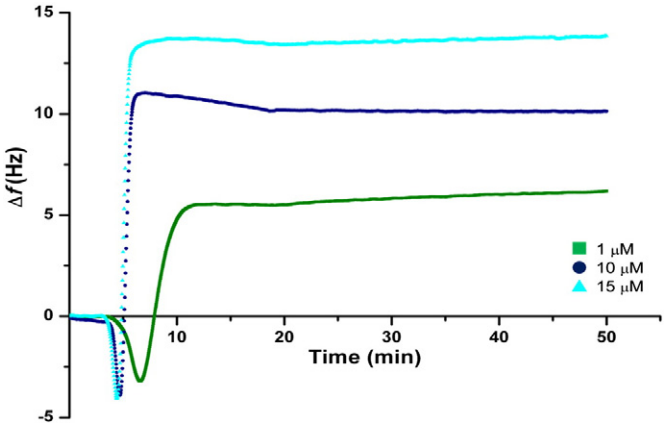

Fig. 3. Δf-t traces from the QCM-D monitoring of the interaction of neomycin B with a DMPC/DMPG (4:1) membrane showing the effect of concentration on membrane uptake.

observed for kanamycin A, membrane disruption was greatest at the highest concentration studied (15 μM), as shown in Fig. 3.

QCM-D experiments are also able to provide depth profiling via analysis of frequency changes at different harmonics of the QCM-D sensor [51,53–55]. Each harmonic probes a defined distance away from the surface of the sensor. This distance is inversely proportional to the frequency of the harmonic [64]. For example, the higher harmonics (7th and 9th) probe close to the sensor surface, whereas the lower harmonics (3rd and 5th) probe further away. Thus, probing the harmonics in a QCM-D experiment can provide a method to assess the nature of the interaction of the aminoglycoside with the membrane layer, i.e., surface vs. trans-membrane binding. The spread of the harmonics (from the 3rd to the 9th) in Δf — t and ΔD — t plots for neomycin B (1–15 μM) and kanamycin A (10 and 15 μM) was similar, as illustrated in Fig. 4 where the 3rd, 5th, 7th and 9th harmonics are shown. This initial overview illustrates the similarities between kanamycin and neomycin in terms of their interaction with the membrane layer. The Δf — t data for kanamycin (Fig. 4a) and neomycin (Fig. 4b) both show a decrease in frequency to ~5 Hz, with overlap of the harmonics. Thus, the initial phase of the aminoglycoside–membrane interaction is independent of the distance from the sensor, consistent with mass addition equally across the membrane, i.e., in a *trans*-membrane fashion. However, in the second phase, beginning at ~5 min, there is the loss of mass (Δf increases) from the sensor, which is characterized by a differential response depending on the harmonic used to sense the frequency. Thus, the 3rd harmonic, which probes the furthest distance, shows the largest increase in frequency, whereas the 9th harmonic plots displayed the lowest increments (Fig. 4). In the second phase, more mass is being removed from the surface of the membrane.

Similar trends were observed for the ΔD — t plots shown in Fig. 4(c) and (d). In these cases, the largest decrease in dissipation was observed for the 3rd harmonic, with progressively smaller decreases in dissipation energy found for higher harmonics. These decreases in ΔD are consistent with a loss of membrane (or aminoglycoside–membrane materials), since the sensor would be expected to become less viscoelastic in response to membrane loss. The data provided by the different harmonics indicate more material being removed from the membrane surface with time, resulting in a decrease in membrane thickness.

Returning to the kanamycin data obtained at 1 μM concentration, only a small displacement of the 3rd harmonic is observed, with the other harmonics almost overlapping (Fig. 5). As discussed above for the initial process, the overlapping harmonics suggest that the added aminoglycoside is inserting in a *trans*-membrane manner, however the displacement of the 3rd harmonic suggests that the surface of the membrane is affected slightly differently. There is always the possibly

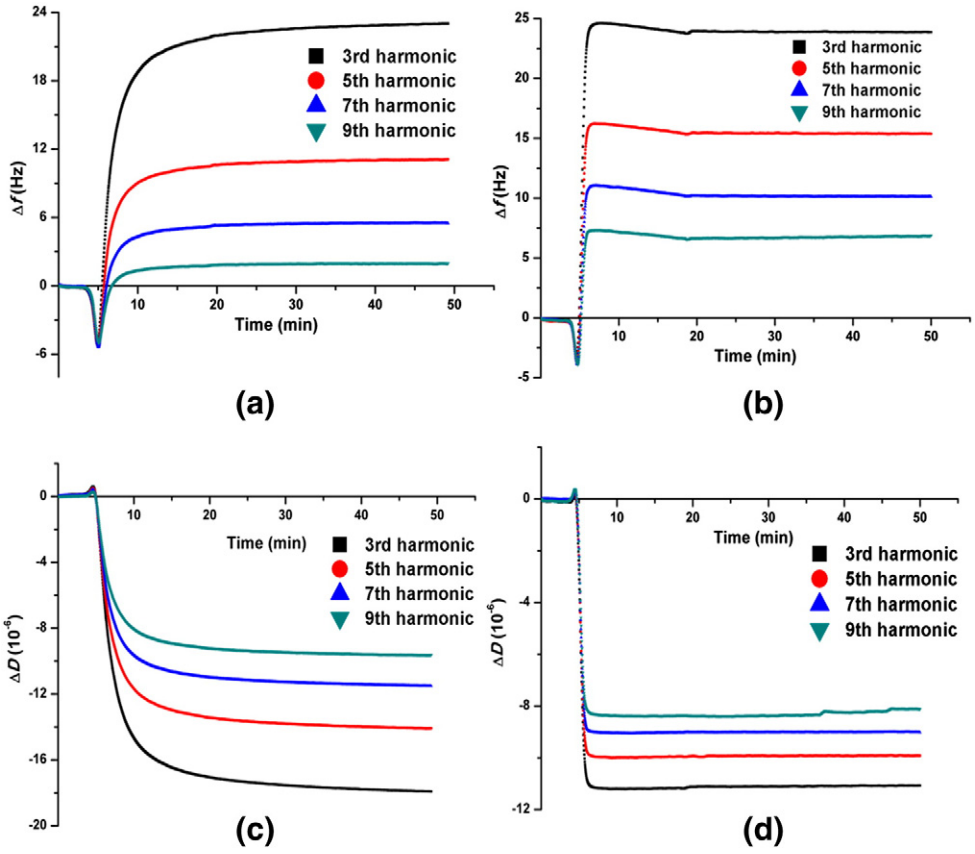

Fig. 4. QCM-D monitoring of kanamycin A (10 μM); (a) Δ*f*-t; (c) Δ*D*-t plots, and neomycin B (10 μM); (b) Δ*f*-t; (d) Δ*D*-t traces, showing the uptake on a DMPC/DMPG (4:1) bacterial mimetic membranes. The response of the 3rd, 5th, 7th and 9th harmonics of the QCM-D sensors are each shown in these panels.

that the membrane surface is somewhat irregular. For example, embedded liposomes could be present that did not burst during the membrane deposition. However, the small but clear harmonic effect observed in the Δ*D* — t values suggests that a two-phase process similar to that observed with the higher aminoglycoside concentrations is occurring. Thus, the responses of the harmonics shown in Fig. 5b (maxima followed by decreases in Δ*D* — t values) are consistent with insertion of kanamycin into the membrane, albeit with slightly more binding occurring at the surface of the membrane, followed by a small loss of material from the surface and a loosening of the membrane layer. It appears that the data in Fig. 5 were captured at just the right concentration for the concentration threshold interaction to be observed.

The temporal frequency and dissipation changes can be combined as Δ*f*-Δ*D* traces to provide greater insight into changes in the structural integrity of the lipid bilayer occurring during mass addition/removal processes. We have previously shown that these traces provide a unique "fingerprint" characteristic of the mode of interaction of a small molecule or biomolecule with the supported phospholipid bilayer-modified sensor [51,53,54,65]. The Δ*f*-Δ*D* fingerprints for both kanamycin A and neomycin B are shown in Fig. 6 (7th harmonic data shown only).

In these plots, the origin represents the starting point for both aminoglycosides. Initially, the binding of each compound is indicated by the observed frequency decrease, i.e., the trace moves from the origin to a maximum value, or 'turning point', that appears characteristic of

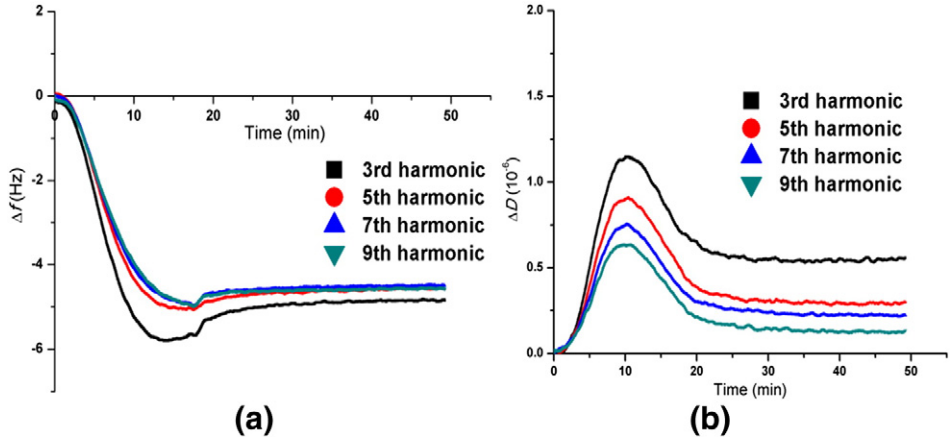

Fig. 5. QCM-D monitoring of kanamycin A (1 μM) uptake on a DMPC/DMPG (4:1) membrane with (a) Δ*f*-t and (b) Δ*D*-t plots showing the effect on the 3rd, 5th, 7th and 9th harmonics.

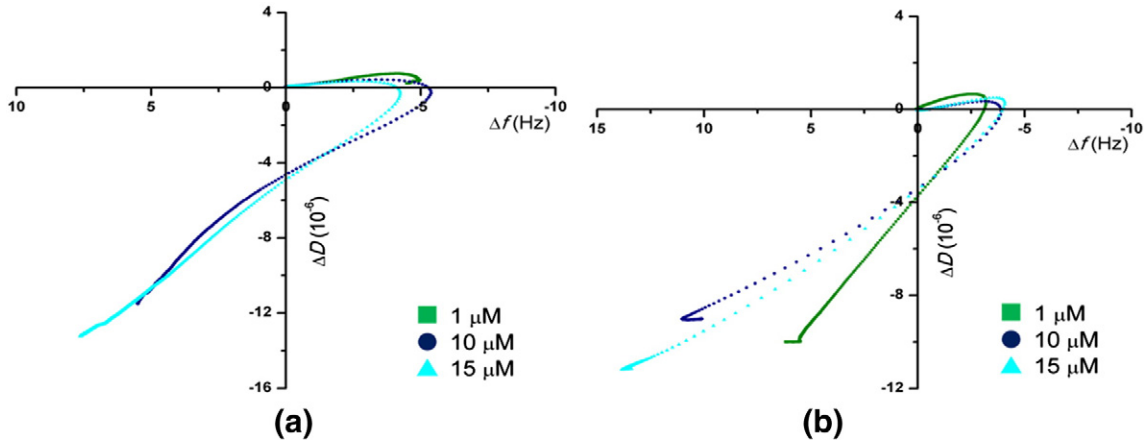

Fig. 6. Energy dissipation (ΔD) *vs.* frequency (Δf) dependence of the interaction of (a) kanamycin A and (b) neomycin B with a DMPC/DMPG (4:1) membrane. The x- and y-axis represent Δf and ΔD (10^{-6}) values, respectively.

each aminoglycoside (its concentration threshold). These traces then almost reverse in direction and continue towards the lower quadrant (positive frequency and negative dissipation region), indicating a loss of materials from the sensor. In summary, the interaction between these aminoglycosides and the model phospholipid membrane is biphasic in nature. The initial decrease in Δf, with minimal changes in ΔD values, followed by a large decrease in ΔD along with an increase in Δf values is characteristic of *trans*-membrane insertion followed by membrane disruption.

Qualitative evaluation of the rates of association/dissociation of kanamycin A and neomycin B was also carried out via time dependent analysis of the first-order derivative of the $\Delta f - t$ curves ($\partial\Delta f/\partial t$ vs. t). These kinetic profiles are shown in Fig. 7 for two concentrations (1 and 10 μM) of each of the aminoglycosides and over the period of time in which material addition and removal processes occurred. These derivative traces reveal an extremely slow mass uptake (<1 Hz/min) of kanamycin A at 1 μM concentration, with the rate of mass addition increasing in the order kanamycin A (1 μM) ≪ neomycin B (1 μM) < kanamycin A (10 μM) ≈ neomycin B (10 μM). At the higher concentrations of kanamycin A and neomycin B, removal of the material from membrane was *ca.* 3-fold faster for neomycin B compared to kanamycin A. Interestingly, at 10 μM concentration, the initial insertion step occurred at a similar rate for both aminoglycosides (~7 Hz/min), whereas the disruption that followed was faster for neomycin B (~20 Hz/min) compared to kanamycin A (~7 Hz/min). The data for neomycin B at 1 μM also showed a similar trend, with the rate of disruption approximately two times greater than the rate of insertion into the membrane.

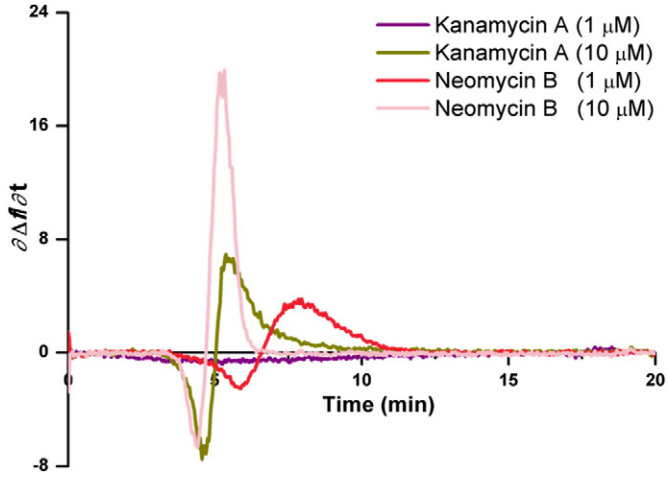

Fig. 7. First-order derivative of 7th harmonic Δf-t traces *vs.* time for the interaction of 10 μM kanamycin A and neomycin B with a DMPC/DMPG (4:1) membrane, as plotted against time. Data for time ≥ 20 min has been omitted for clarity.

Both kanamycin A (+4) and neomycin B (+6) are positively charged at pH = 6.90. Thus, the initial rapid association and insertion into the lipid membrane could be due to strong electrostatic attraction with the anionic membrane surface (DMPC/DMPG (4:1)). In addition, the DMPG component contains a glycerol group that could assist in hydrogen-bonding interactions with the cationic aminoglycosides, although we have no direct evidence of these interactions. The associative binding of the aminoglycosides is not a favorable interaction in the membrane, and we believe that local disorder in the lipid bilayer results, followed by removal of material. Thus, disruption of bacterial mimetic DMPC/DMPG (4:1) membrane by kanamycin A and neomycin B is a biphasic process, as illustrated in Fig. 8 [53–55,66]. The individual polycationic aminoglycoside molecules insert into the membrane surface in a *trans*-membrane orientation, until a threshold concentration is reached, whereupon the combined interactions between the molecules and the lipid membrane (electrostatics, hydrogen-bonding) result in destabilization of the membrane and accretion of material.

4. Conclusion

QCM-D analysis indicates that the two well-known aminoglycosides, kanamycin A and neomycin B, interact with a bacterial mimetic membrane (DMPC/DMPG (4:1)) via a two-stage mechanism. Initial aminoglycoside insertion into the membrane is rapid and occurs in a trans-membrane fashion. This is followed by an equally facile membrane disruption stage once a critical concentration threshold is reached. Loss of membrane material occurs more from the surface of the membrane than the interior. Kanamycin A and neomycin B both show similar rates of insertion into the anionic membrane surface, however they differ slightly in their rates of membrane disruption. Neomycin B causes a greater degree of membrane disruption, which is argued to be due to its greater cationic charge. It is hypothesized that electrostatic interactions of the polycationic aminoglycoside with the anionic membrane surface and intermolecular hydrogen-bonding interactions between the lipid membrane and the charged aminoglycoside molecules contribute to local disorder and stress within the lipid bilayer, leading to the membrane damage and removal of material. If this is indeed the case, incorporation of functional groups to enhance these interactions could produce compounds with enhanced potency, which might serve as the basis for new antimicrobial therapeutic treatments urgently needed to combat the rapid growing population of drug-resistant viruses and bacteria. With this in mind, we are currently

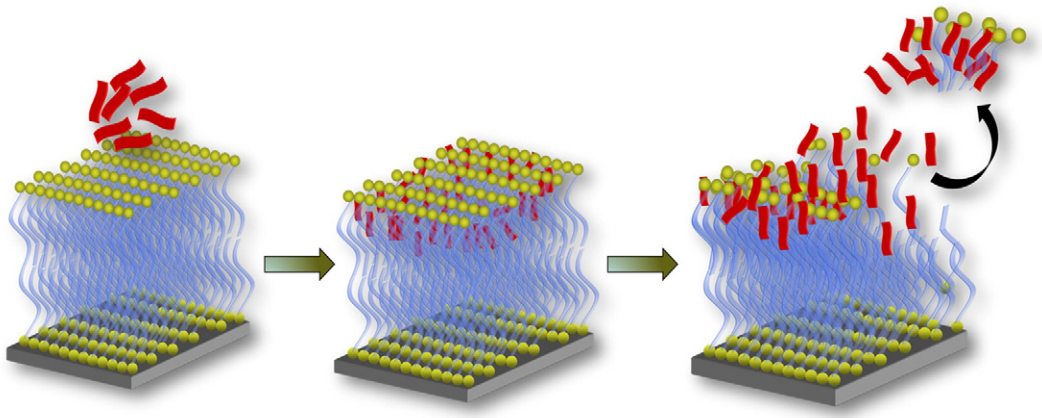

Fig. 8. Proposed biphasic mode-of-action for kanamycin A and neomycin B (represented as red ribbons) on DMPC/DMPG (4:1) lipid membranes (yellow-blue ribbons). The mechanism for these aminoglycosides is initially insertion, followed by disruption of the membrane layer.

conducting in-depth QCM-D investigations of the interactions of several such modified aminoglycoside derivatives with bacterial mimetic membranes.

Abbreviations

DMPC	1,2-dimyristoyl-sn-glycero-3-phosphocholine
DMPG	1,2-dimyristoyl-sn-glycero-3-phospho-rac-(1-glycerol)
DOS	2-deoxystreptamine
MDR	Multi-drug resistance
MPA	3-mercaptopropionic acid
QCM-D	Quartz Crystal Microbalance with Dissipation monitoring
RNA	Ribonucleic acid

Acknowledgements

This work was financially supported by the Australian Research Council through the Discovery Program (LS and LLM) and a Future Fellowship to BG (FT130100838). TJ was a recipient of Monash Graduate Scholarship (MGS), Monash International Postgraduate Research Scholarship (MIPRS) and Postgraduate Publication Award (PPA).

Appendix A. Supplementary data

Supplementary data to this article can be found online at http://dx.doi.org/10.1016/j.bbamem.2014.10.019.

References

[1] R.J. Fair, M.E. Hensler, W. Thienphrapa, Q.N. Dam, V. Nizet, Y. Tor, ChemMedChem 7 (2012) 1237–1244.
[2] L.S. Gonzalez III, J.P. Spencer, Am. Fam. Physician 58 (1998) 1811–1820.
[3] G.L. Drusano, Clin. Infect. Dis. 45 (2007) S89–S95.
[4] H.W. Boucher, G.H. Talbot, J.S. Bradley, J.E. Edwards, D. Gilbert, L.B. Rice, M. Scheld, B. Spellberg, J. Bartlett, Clin. Infect. Dis. 48 (2009) 1–12.
[5] D.J. Payne, M.N. Gwynn, D.J. Holmes, D.L. Pompliano, Nat. Rev. Drug Discov. 6 (2007) 29–40.
[6] B. Walker, S. Barrett, S. Polasky, V. Galaz, C. Folke, G. Engström, F. Ackerman, K. Arrow, S. Carpenter, K. Chopra, G. Daily, P. Ehrlich, T. Hughes, N. Kautsky, S. Levin, K.-G. Mäler, J. Shogren, J. Vincent, T. Xepapadeas, A. de Zeeuw, Science 325 (2009) 1345–1346.
[7] J.S. Bradley, R. Guidos, S. Baragona, J.G. Bartlett, E. Rubinstein, G.G. Zhanel, M.D. Tino, D.L. Pompliano, F. Tally, P. Tipirneni, G.S. Tillotson, J.H. Powers, Lancet Infect. Dis. 7 (2007) 68–78.
[8] B. Spellberg, M. Blasser, R.J. Guidos, H.W. Boucher, J.S. Bradley, B.I. Eisenstein, D. Gerding, R. Lynfield, L.B. Reller, J. Rex, D. Schwartz, E. Septimus, F.C. Tenover, D.N. Gilbert, Clin. Infect. Dis. 52 (2011) S397–S428.
[9] L. Yang, X.S. Ye, Curr. Top. Med. Chem. 10 (2010) (1898-1826).
[10] P. Poulikakos, M.E. Falagas, Expert Opin. Pharmacother. 14 (2013) 1585–1597.
[11] R. Maviglia, R. Nestorini, M. Pennisi, Curr. Drug Targets 10 (2009) 895–905.
[12] J. Jackson, C. Chen, K. Buising, Curr. Opin. Infect. Dis. 26 (2013) 516–525.
[13] J.L. Houghton, K.D. Green, W. Chen, S. Garneau-Tsodikova, ChemBioChem 11 (2010) 880–902.
[14] P. Dozzo, H.E. Moser, Expert Opin. Ther. Pat. 20 (2010) 1321–1341.
[15] B. Becker, M.A. Cooper, ACS Chem. Biol. 8 (2013) 105–115.
[16] M. Bassetti, M. Merelli, C. Temperoni, A. Astilean, Ann. Clin. Microbiol. Antimicrob. 12 (2013) 22.
[17] M. Bassetti, F. Ginocchio, M. Mikulska, L. Taramasso, D.R. Giacobbe, Expert Rev. Anti-Infect. Ther. 9 (2011) 909–922.
[18] C.B. Landersdorfer, N.S. Ly, H. Xu, B.T. Tsuji, J.B. Bulitta, Antimicrob. Agents Chemother. 57 (2013) 2343–2351.
[19] Y. Tor, ChemBioChem 4 (2003) 998–1007.
[20] J.J. Comroe, Am. Rev. Respir. Dis. 117 (1978) 773–781.
[21] R. Schroeder, C. Waldsich, H. Wank, EMBO J. 19 (2000) 1–9.
[22] Y. Tor, ChemInform (1999) 30.
[23] J. Gallego, G. Varani, Acc. Chem. Res. 34 (2001) 836–843.
[24] H. Wank, E. Clodi, M.G. Wallis, R. Schroeder, Orig. Life Evol. Biosph. 29 (1999) 391–404.
[25] D.W. Staple, V. Venditti, N. Niccolai, L. Elson-Schwab, Y. Tor, S.E. Butcher, ChemBioChem 9 (2008) 93–102.
[26] W.K.C. Park, M. Auer, H. Jaksche, C.-H. Wong, J. Am. Chem. Soc. 118 (1996) 10150–10155.
[27] W. Wang, Z. Guo, Y. Chen, T. Liu, L. Jiang, Chem. Biol. Drug Des. 68 (2006) 314–318.
[28] H. Zhao, J. Li, L. Jiang, Biochem. Biophys. Res. Commun. 320 (2004) 95–99.
[29] S.R. Kirk, Y. Tor, Chem. Commun. (1998) 147–148.
[30] M.J. Belousoff, B. Graham, L. Spiccia, Y. Tor, Org. Biomol. Chem. 7 (2009) 30–33.
[31] S. Lodhi, N.D. Weiner, J. Schacht, Biochim. Biophys. Acta Biomembr. 426 (1976) 781–785.
[32] G. laurent, M.-B. Carlier, B. Rollman, F. Van Hoof, P. Tulkens, Biochem. Pharmacol. 31 (1982) 3861–3870.
[33] S. Lodhi, N.D. Weiner, I. Mechigian, J. Schacht, Biochem. Pharmacol. 29 (1980) 597–601.
[34] M.W. Yung, C. Green, Biochem. Pharmacol. 35 (1986) 4037–4041.
[35] A.J. Duvall, K.S. Robinson, S.J. Feist, Eur. Arch. Otorhinolaryngol. 248 (1991) 319–325.
[36] P.R. Langford, E.S. Harpur, J.B. Kayes, I. Gonda, J. Antibiot. (Tokyo) 35 (1982) 1387–1393.
[37] H.H. Zepik, P. Walde, E.L. Kostoryz, J. Code, D.M. Yourtee, Crit. Rev. Toxicol. 38 (2008) 1–11.
[38] R.E.W. Hancock, J. Antimicrob. Chemother. 8 (1981) 429–445.
[39] R.E.W. Hancock, J. Antimicrob. Chemother. 8 (1981) 249–276.
[40] M.P. Mingeot-LeClercq, A. Schanck, M.F. Ronveaux-Dupal, M. Deleers, R. Brasseur, J.M. Ruysschaert, G. Laurent, P.M. Tulkens, Biochem. Pharmacol. 38 (1989) 729–741.
[41] G.J. Kaloyanides, Ren. Fail. 14 (1992) 351–357.
[42] F. van Bambeke, M.-P. Mingeot-Leclercq, R. Brasseur, P.M. Tulkens, A. Schanck, Chem. Phys. Lipids 79 (1996) 123–135.
[43] K. Iida, M. Koike, Antimicrob. Agents Chemother. 5 (1974) 95–97.
[44] H.W. Taber, J.P. Mueller, P.F. Miller, A.S. Arrow, Microbiol. Mol. Biol. Rev. 51 (1987) 439–457.
[45] T. Montie, P. Patamasucon, Eur. J. Clin. Microbiol. Infect. Dis. 14 (1995) 85–87.
[46] R.E. Hancock, S.W. Farmer, Z.S. Li, K. Poole, Antimicrob. Agents Chemother. 35 (1991) 1309–1314.
[47] R.A. Moore, W.A. Woodruff, R.E. Hancock, Antibiot. Chemother. 39 (1987) 172–181.
[48] S.B. Nielsen, D.E. Otzen, in: J.H. Kleinschmidt (Ed.), Lipid-Protein Interactions, vol. 974, Humana Press, 2013, pp. 1–21.
[49] R.E. Speight, M.A. Cooper, J. Mol. Recognit. 25 (2012) 451–473.
[50] A. Mechler, S. Praporski, S. Piantavigna, S.M. Heaton, K.N. Hall, M.-I. Aguilar, L.L. Martin, Biomaterials 30 (2009) 682–689.
[51] T. Joshi, G. Gasser, L.L. Martin, L. Spiccia, RSC Adv. 2 (2012) 4703–4712.

[52] T.K. Lind, M. Cárdenas, H.P. Wacklin, Langmuir 30 (2014) 7259–7263.
[53] S. Piantavigna, G.A. McCubbin, S. Boehnke, B. Graham, L. Spiccia, L.L. Martin, Biochim. Biophys. Acta Biomembr. 1808 (2011) 1811–1817.
[54] G. McCubbin, S. Praporski, S. Piantavigna, D. Knappe, R. Hoffmann, J. Bowie, F. Separovic, L. Martin, Eur. Biophys. J. 40 (2011) 437–446.
[55] A. Mechler, S. Praporski, K. Atmuri, M. Boland, F. Separovic, L.L. Martin, Biophys. J. 93 (2007) 3907–3916.
[56] J.B. Dame, B.M. Shapiro, J. Bacteriol. 137 (1979) 1043–1047.
[57] C.S.B. Chia, J. Torres, M.A. Cooper, I.T. Arkin, J.H. Bowie, FEBS Lett. 512 (2002) 47–51.
[58] G. van Meer, D.R. Voelker, G.W. Feigenson, Nat. Rev. Mol. Cell Biol. 9 (2008) 112–124.
[59] S.E. Blondelle, K. Lohner, M.I. Aguilar, Biochim. Biophys. Acta Biomembr. 1462 (1999) 89–108.
[60] G. Sauerbrey, Z. Phys. 155 (1959) 206–222.
[61] M. Rodahl, F. Hook, C. Fredriksson, C.A. Keller, A. Krozer, P. Brzezinski, M. Voinova, B. Kasemo, Faraday Discuss. 107 (1997) 229–246.
[62] M.C. Dixon, J. Biomol. Tech. 19 (2008) 151–158.
[63] N.-J. Cho, K.K. Kanazawa, J.S. Glenn, C.W. Frank, Anal. Chem. 79 (2007) 7027–7035.
[64] M. Rodahl, B. Kasemo, Sensors Actuators A Phys. 54 (1996) 448–456.
[65] P.J. Sherman, R.J. Jackway, J.D. Gehman, S. Praporski, G.A. McCubbin, A. Mechler, L.L. Martin, F. Separovic, J.H. Bowie, Biochemistry 48 (2009) 11892–11901.
[66] Y. Shai, Biochim. Biophys. Acta Biomembr. 1462 (1999) 55–70.